

Geophysical Research Letters[®]



RESEARCH LETTER

10.1029/2023GL103188

Tug-Of-War on Idealized Midlatitude Cyclones Between Radiative Heating From Low-Level and High-Level Clouds

Aiko Voigt¹ , Behrooz Keshtgar² , and Klara Butz¹

¹Department of Meteorology and Geophysics, University of Vienna, Vienna, Austria, ²Institute of Meteorology and Climate Research—Department Troposphere Research, Karlsruhe Institute of Technology, Karlsruhe, Germany

Key Points:

- Radiative heating from high clouds leads to a stronger cyclone, radiative heating from low clouds leads to a weaker cyclone
- Because of this tug-of-war, the overall effect of cloud-radiative heating can be a stronger or weaker cyclone
- The radiative impact of clouds can be understood from the effect on static stability

Supporting Information:

Supporting Information may be found in the online version of this article.

Correspondence to:

A. Voigt,
aiko.voigt@univie.ac.at

Citation:

Voigt, A., Keshtgar, B., & Butz, K. (2023). Tug-of-war on idealized midlatitude cyclones between radiative heating from low-level and high-level clouds. *Geophysical Research Letters*, 50, e2023GL103188. <https://doi.org/10.1029/2023GL103188>

Received 10 FEB 2023
Accepted 22 JUN 2023

Author Contributions:

Conceptualization: Aiko Voigt
Data curation: Aiko Voigt
Formal analysis: Aiko Voigt, Klara Butz
Funding acquisition: Aiko Voigt
Investigation: Aiko Voigt, Behrooz Keshtgar, Klara Butz
Methodology: Aiko Voigt, Behrooz Keshtgar
Project Administration: Aiko Voigt
Resources: Aiko Voigt
Software: Aiko Voigt, Behrooz Keshtgar, Klara Butz
Supervision: Aiko Voigt, Behrooz Keshtgar
Visualization: Aiko Voigt, Klara Butz
Writing – original draft: Aiko Voigt

Abstract We present baroclinic life-cycle simulations with two versions of the atmosphere model ICON to understand how cloud-radiative heating and cooling affect an idealized midlatitude cyclone. Both versions simulate the same cyclone when run without radiation, but disagree when cloud-radiation-interaction is taken into account. The radiative effects of clouds weaken the cyclone in ICON2.1 but strengthen it in ICON2.6. We attribute the disagreement to low-level clouds, which in ICON2.1 are more abundant and show stronger radiative cooling of the boundary layer. We argue that radiative cooling from low-level cloud tops weakens the cyclone by increasing boundary-layer static stability, and that radiative cooling from high-level cloud tops strengthens the cyclone by decreasing static stability in the upper troposphere and sharpening the tropopause. Our results indicate that clouds and the vertical distribution of their radiative heating and cooling can influence the dynamics of midlatitude cyclones.

Plain Language Summary The interaction of tiny cloud particles with even smaller photons leads to cooling and heating of the atmosphere. We use computer simulations to show that this cloud-radiative cooling and heating changes the intensity of a midlatitude low-pressure system. Clouds near the surface lead to a less intense low-pressure system, while clouds in the upper troposphere, about 10 km above the surface, strengthen the low-pressure system.

1. Introduction

“All models are wrong. Some are wrong in useful ways.” (adapted by the authors from Box, 1979) In this paper, we take advantage of an error in the ICON atmosphere model to elucidate how cloud-radiative heating and cooling affects the intensity of idealized midlatitude cyclones. For brevity, we will in the following use the term cloud-radiative heating, independent of its sign.

Midlatitude cyclones are an important part of the atmospheric circulation. On time scales of days, they determine midlatitude weather and influence weather extremes (Shapiro & Gronas, 1999) and have been a topic of weather research for many decades (Schultz et al., 2019). In particular, numerous studies have been conducted to understand how latent heating, convection and cloud microphysics affect midlatitude cyclones and the jet stream along which they propagate (e.g., Ahmadi-Givi, 2002; Crezee et al., 2017; Davis et al., 1993; Pfahl et al., 2015).

On climate time scales of years, midlatitude cyclones dominate the redistribution of energy, moisture and momentum from the subtropics to higher latitudes (Shaw et al., 2016). As such, they are essential to the planetary-scale circulation of the atmosphere. Work with a focus on climate has highlighted how the interactions of cloud particles with radiation shape the position of the planetary-scale circulation in the present-day climate (Li et al., 2015; Watt-Meyer & Frierson, 2017) and its response to climate change (e.g., Albern et al., 2019, 2021; Ceppi & Hartmann, 2016; Grise & Polvani, 2014; Voigt et al., 2019; Voigt & Shaw, 2015). The impact arises from the spatiotemporal pattern of cloud-radiative heating in the atmosphere and at the surface, and is thought to be critical to the response of the midlatitude jet stream and storm tracks as the Earth warms (Voigt et al., 2021).

The distinction between weather and climate time scales has led to the perception that latent heating dominates on weather time scales, while radiative heating dominates on climate time scales, provided that the effect of latent heating on static stability is taken into account (O’Gorman, 2011). This perception is reflected in the weather community’s view of radiation as a slow process, and the climate community’s view of convection as a quasi-instantaneous process that restores the atmosphere to neutral conditions in response to radiative destabilization.

© 2023. The Authors.

This is an open access article under the terms of the [Creative Commons Attribution License](https://creativecommons.org/licenses/by/4.0/), which permits use, distribution and reproduction in any medium, provided the original work is properly cited.

Writing – review & editing: Aiko Voigt, Behrooz Keshtgar, Klara Butz

The view that radiation is a slow process of minor importance in the evolution of weather events is changing, however. For example, tropical cyclones are understood to be enhanced by contrasts in longwave cloud-radiative heating (Ruppert et al., 2020). Chagnon et al. (2013) showed that the contrast between the moist troposphere and the dry stratosphere creates radiative heating around the tropopause that sharpens gradients in potential vorticity. Grise et al. (2019) argued that the collocation of cloud-radiative heating with the wind field of cyclones leads to weaker midlatitude cyclones. Consistent with this, Schäfer and Voigt (2018) reported that idealized cyclones are weakened by cloud-radiative heating. Inconsistent with this, however, Keshtgar et al. (2023) argued that idealized cyclones are strengthened by cloud-radiative heating.

In this paper, we show that cloud-radiative heating can have a strengthening or weakening effect on idealized midlatitude cyclones depending on the vertical distribution of clouds and their radiative heating inside the atmosphere. To this end, we perform baroclinic life-cycle simulations in which we include the effects of both latent heating and cloud-radiative heating. Remarkably, the effect of radiation was ignored in the past, apart from a few exceptions. We identified more than 100 peer-reviewed publications that applied baroclinic life cycle simulations of idealized midlatitude cyclones. Of these, only six included radiation (Kaviani et al., 2022; Keshtgar et al., 2023; Kunkel et al., 2016, 2019; Schäfer & Voigt, 2018; Volonté et al., 2020), and only Keshtgar et al. (2023) and Schäfer and Voigt (2018) examined the impact of cloud-radiative heating. These numbers speak to the need to better understand how radiation in general, and cloud-radiation interactions in particular, shape the development of midlatitude cyclones.

2. Methods and Simulation Setup

We use the ICON global atmosphere model (Zängl et al., 2015) with the physics parameterization package for numerical weather prediction (ICON-NWP; Prill et al., 2020). We use the same 40 km horizontal grid spacing (R2B06 grid), 90 vertical levels and physics settings as the baroclinic life-cycle simulation presented in Schäfer and Voigt (2018). This includes the 1-moment cloud microphysics scheme of Doms et al. (2011) and the RRTM radiation scheme (Barker et al., 2003; Mlawer et al., 1997).

The initial and boundary conditions are typical for baroclinic life-cycle simulations (e.g., Booth et al., 2013; Rantanen et al., 2019; Tierney et al., 2018) and taken from Schäfer and Voigt (2018), who adapted them from the type-1 lifecycle setup of Polvani and Esler (2007). ICON is configured as an aquaplanet with no sea ice and prescribed time-constant sea-surface temperatures. Sea-surface temperatures are 0.5 K lower than the initial temperature of the lowest model level. The initial meridional wind, vertical wind and cloud fields are zero. The initial zonal wind and temperature describe a zonally uniform atmosphere in thermal wind balance with a baroclinically unstable jet stream at 45°N. Baroclinic growth is induced by a wavenumber-6 temperature perturbation of 1 K amplitude at the latitude of the jet. This results in the development of a set of 6 cyclones; for the analysis we average over the 6 cyclones.

The cyclones grow in a moist atmosphere with initial relative humidity

$$RH = RH_0 \cdot (1 - 0.85 \cdot z/z_T)^{5/4}, \quad (1)$$

where $RH_0 = 80\%$ and $z_T = 12$ km. Above $z = 14$ km, the initial RH is zero and the atmospheric composition in terms of non-condensable trace gases (e.g., CO_2 , CH_4) is as in Schäfer and Voigt (2018).

We run two versions of ICON that, as we will see in Section 3, disagree on the impact of cloud-radiative heating on the cyclone. The first version is ICON2.1.00 (hereafter ICON2.1). ICON2.1 differs from the model version 2.0.15 used in Schäfer and Voigt (2018) only in terms of minor technical changes and closely reproduces the results of Schäfer and Voigt (2018) (Figures S1, S2 and S3 in Supporting Information S1). The German Weather Service DWD introduced version 2.0.15 as its operational forecast model in September 2016 (Zängl & Paul, 2016).

The second version is ICON2.6.2.2 (hereafter ICON2.6). ICON2.6 was used by Keshtgar et al. (2023) for baroclinic life-cycle simulations in an extratropical channel setup and was introduced as the operational model at DWD in April 2021 (Zängl, 2021). It differs from ICON2.1 in the correction of a major model error in the physics-dynamics coupling (Rieger et al., 2021; Zängl & Schäfer, 2021). In ICON2.1, the heat capacity of air at constant pressure, c_p , is used to convert the turbulent heat flux into an atmospheric temperature tendency. However, because ICON is based on height levels, the conversion requires the heat capacity of air at constant volume, c_v . The error became known as the “ $c_p/c_v = 1.4$ bug” and was fixed in ICON2.6. As described in the Section 3, the

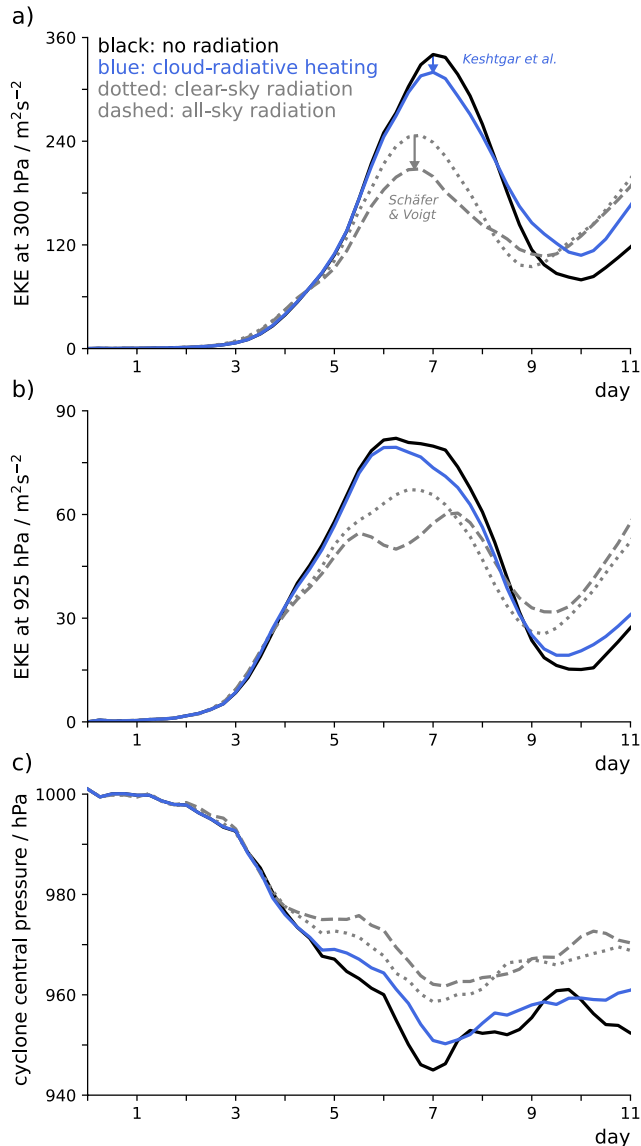


Figure 1. Time series of cyclone intensity metrics for different treatments of radiation in ICON2.1. Eddy kinetic energy (EKE) is averaged between 25° and 75°N , which covers the region where the cyclone is developing. The blue arrow shows the cloud-radiative impact diagnosed by the method of Keshtgar et al. (2023), the gray arrow shows the impact diagnosed by the method of Schäfer and Voigt (2018). Note that the difference between the no-radiation and clear-sky simulations as well as the difference between the simulations with cloud-radiative heating and all-sky radiation provide an estimate of the impact of clear-sky radiative heating, which is not the topic of this study.

of lower-level EKE changes from a single peak for clear-sky radiation to a double peak when cloud-radiative heating is included. This indicates qualitative changes in the dynamics of the cyclone that, while interesting, may complicate the interpretation of the cloud-radiative impact. This complication does not occur with the method of Keshtgar et al. (2023).

3.1. Conflicting Impact of Cloud-Radiative Heating in ICON2.1 and ICON2.6

The cloud-radiative impact is fundamentally different between ICON2.1 and ICON2.6, as shown in Figure 2. While in ICON2.1 cloud-radiative heating leads to a weaker cyclone, in ICON2.6 the cyclone becomes stronger in terms

error results in a warmer and moister boundary layer in ICON2.1 compared to ICON2.6, and strong differences in low-level clouds and cloud-radiative heating between the two model versions.

Previous work used different methods to diagnose the cloud-radiative impact. Schäfer and Voigt (2018) estimated the impact from the difference between two simulations driven by all-sky and clear-sky radiation, respectively. Keshtgar et al. (2023) proposed an alternative method and estimated the cloud-radiative impact from the difference between a simulation with no radiation and a simulation in which cloud-radiative heating of the atmosphere is taken into account but clear-sky radiative heating is not. This is achieved by passing the cloud-radiative heating to the dynamical core instead of the all-sky radiative heating. Cloud-radiative heating is given by

$$\frac{\partial T}{\partial t} \Big|_{\text{radiation}}^{\text{cloud}} = \frac{\partial T}{\partial t} \Big|_{\text{radiation}}^{\text{all-sky}} - \frac{\partial T}{\partial t} \Big|_{\text{radiation}}^{\text{clear-sky}} = \frac{1}{\rho c_v} \cdot \frac{\partial}{\partial z} (F^{\text{all-sky}} - F^{\text{clear-sky}}) \quad (2)$$

where ρ is the air density and F is the radiative flux in all-sky and clear-sky conditions. For ICON2.1 we use both methods. When comparing ICON2.1 and ICON2.6 we use the second method for reasons explained in Section 3.

We focus on cyclone intensity, which we characterize in terms of eddy kinetic energy (EKE) and cyclone central pressure. EKE is defined with respect to the zonal-mean wind at a given time step. Cyclone central pressure is the minimum surface pressure within the cyclone region, where we first construct the mean cyclone by averaging over the six individual cyclones.

3. Results

We first show that the cloud-radiative impact on the cyclone is robust to the diagnostic method. For this purpose, we use the ICON2.1 simulations and compare the methods of Schäfer and Voigt (2018) and Keshtgar et al. (2023) in Figure 1. For the method of Keshtgar et al. (2023), the cyclone weakening is less pronounced in terms of EKE (Figures 1a and 1b) but more pronounced in terms of cyclone core pressure (Figure 1c). Despite these quantitative differences, both methods agree that cloud-radiative heating leads to a weaker cyclone.

Throughout the rest of the paper, we will use the Keshtgar et al. (2023) method because it isolates the impact of cloud-radiative heating in a cleaner and easier to interpret way. When the method of Keshtgar et al. (2023) is used, the atmospheric state during the first 3 days hardly changes when cloud-radiative heating is enabled and the cyclone grows in the same background state of zonal-mean temperature and zonal wind in the simulations without radiation and with cloud-radiative heating (Figure S4 in Supporting Information S1). The method of Keshtgar et al. (2023) thus avoids the strong cooling of the atmosphere during the first 3 days due to clear-sky radiation (mainly from water vapor) that occurs in the method of Schäfer and Voigt (2018) (Figure S4 in Supporting Information S1). Furthermore, in simulations using the method of Schäfer and Voigt (2018), the evolution

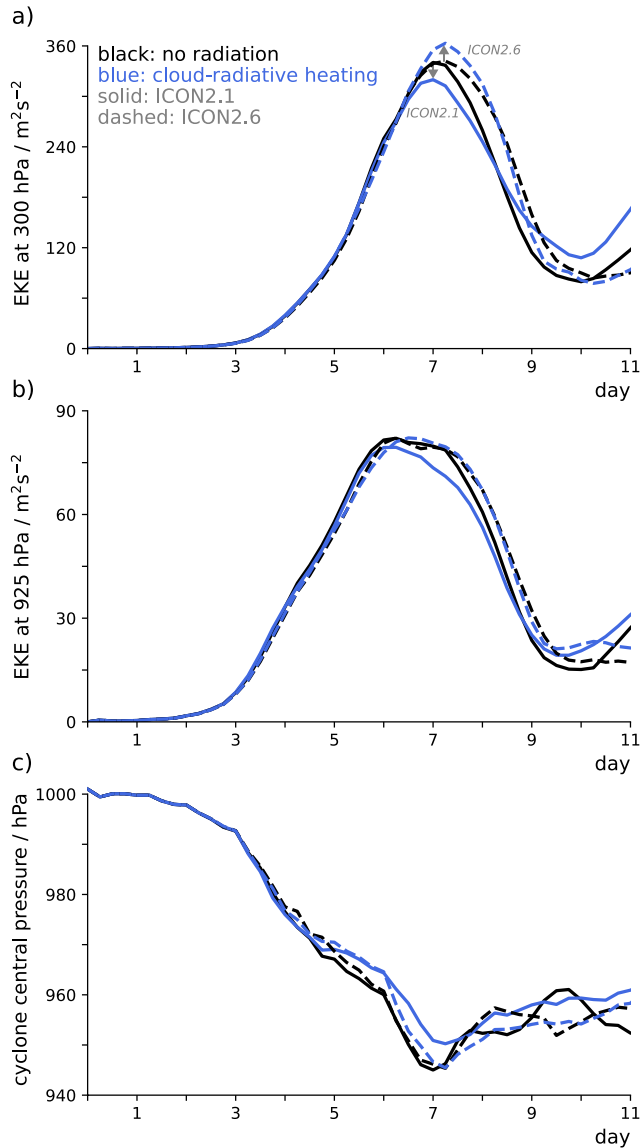


Figure 2. Cloud-radiative impact on the cyclone evolution in terms of (a) EKE at 300 hPa, (b) EKE at 925 hPa and (c) cyclone central pressure for ICON2.1 in solid lines and ICON2.6 in dashed lines. EKE is averaged between 25° and 75°N, which covers the region in which the cyclone develops.

many more low-level clouds, the diagnostic cloud-radiative heating is twice as strong in ICON2.1 around 1.5 km altitude (Figure 3f). In contrast, the diagnostic cloud-radiative heating above the boundary layer is very similar between ICON2.1 and ICON2.6, consistent with the good agreement in cloud ice. The diagnostic cooling around 10 km is the result of longwave emission from the tops of high-level clouds that form as part of the warm conveyor belt of the cyclone (Figure S7 in Supporting Information S1).

The simulations with active cloud-radiative heating exhibit similar differences between ICON2.1 and ICON2.6 with respect to low-level clouds and cloud-radiative heating as the simulations without radiation. This implies that while cloud-radiation-circulation feedbacks might modify the cloud field, these feedbacks are not strong enough to override the principal differences between ICON2.1 and ICON2.6. This confirms that the diagnostic cloud-radiative heating of the no-radiation simulations is indeed useful for understanding the differences between the two model versions.

of upper-level EKE when cloud-radiative heating is included (Figure 2a). The EKE energy changes have the same sign throughout the troposphere (Figure S5 in Supporting Information S1). In ICON2.6 the cloud-radiative impact is close to zero in terms of lower-level EKE and cyclone central pressure (Figures 2b and 2c). Further below, in Section 3.3, we will demonstrate that the conflict between the two model versions results from a robust tug of war between low-level and high-level clouds and model differences in the simulation of low-level clouds.

To put the cloud-radiative impact into perspective, we compare our results to previous simulations of moist baroclinic life cycles based on vertically integrated eddy kinetic energy (integrated over all model levels; Figure S6 in Supporting Information S1). Vertically integrated eddy kinetic energy decreases by 8% in ICON2.1 and increases by 5% in ICON2.6 due to cloud-radiative heating. While the impact of cloud-radiative heating is smaller than that of latent heating (Booth et al., 2013; Schäfer & Voigt, 2018), it is comparable to changes in the zonal wind strength by 10 m/s, a uniform warming by 6 K, or a change in the pole-to-equator temperature contrast by 10 K (Rantanen et al., 2019; Tierney et al., 2018).

Remarkably, ICON2.1 and ICON2.6 simulate essentially the same cyclone when run without radiation. This can be seen from the time series of EKE and cyclone central pressure for the no-radiation simulations in Figure 2 (black lines) and is further illustrated in Figure 3. The two model versions show almost the same surface pressure pattern at day 6 (gray contours in Figures 3a and 3b). However, they differ strongly in the cloud field that is associated with the cyclone (colored shading in Figures 3a and 3b). ICON2.1 simulates many more low-level clouds than ICON2.6, especially in the high-pressure region of the cyclone. Averaged over the cyclone domain from 25° to 75°N, the cloud liquid water content in the planetary boundary layer is two times higher in ICON2.1 (Figure 3c), while cloud ice water content is very similar between the two model versions. The cyclones themselves, however, are not affected by the differences in boundary-layer temperature and moisture.

Panels d–f of Figure 3 show the “diagnostic” cloud-radiative heating of the no-radiation cyclone. “Diagnostic” means that the cloud-radiative heating is calculated during the simulation but not given to the dynamical core of the model and hence does not affect the cyclone.

The strong differences in low-level clouds lead to very different diagnostic cloud-radiative heating in the lower troposphere. In both versions, the diagnostic heating near the top of the boundary layer is negative due to longwave radiative cooling from the tops of low-level clouds in the region of the surface high (Figures 3d and 3e). However, because ICON2.1 simulates

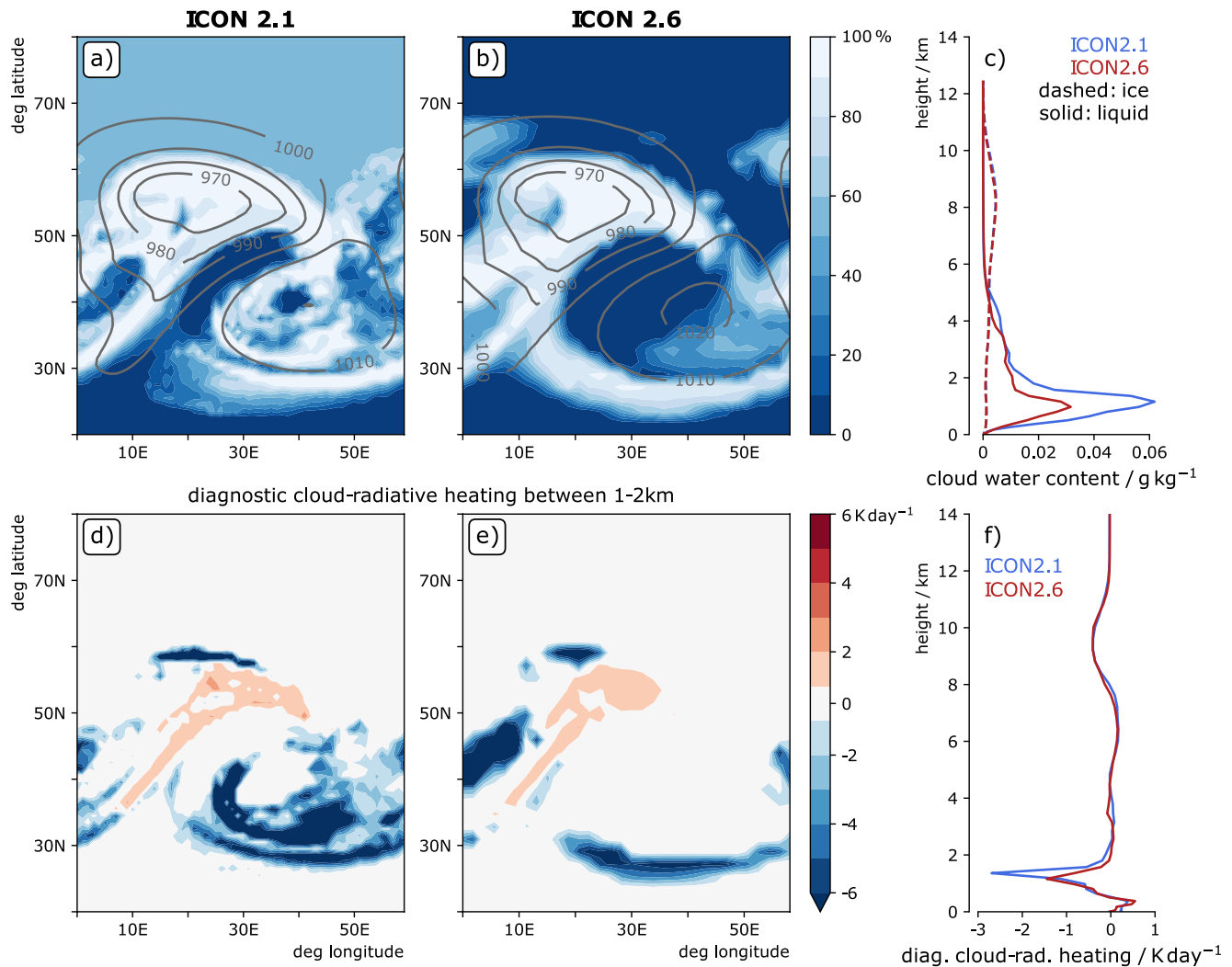


Figure 3. Comparison of clouds and diagnostic cloud-radiative heating in ICON2.1 and ICON2.6 for simulations without radiation on day 6. (a, b) Low-level cloud cover in percent is shown by the filled contours, surface pressure in hPa is shown by the gray contour lines. (c) Vertical distribution of cloud ice water content in dashed lines and cloud liquid water content in solid lines, averaged between 25° and 75°N. (d, e) Boundary-layer diagnostic cloud-radiative heating in K day⁻¹. (f) Vertical distribution of diagnostic cloud-radiative heating averaged between 25° and 75°N.

3.2. Tug-Of-War

Figure 4a shows the cloud-radiative heating in the simulations with cloud-radiative heating, averaged over regions of upward motion between 40° and 60°N and between day 5 and day 6.5. Panel b shows the corresponding temperature change, and panel c the change in static stability. Static stability is calculated as the vertical gradient of potential temperature.

The vertical pattern of cloud-radiative heating has two main components: radiative cooling of the upper part of the boundary layer between 1 and 2 km, and radiative cooling of the upper troposphere near 10 km. The two components result from the emission of longwave radiation from tops of low-level and high-level clouds, respectively. The vertical pattern of cloud-radiative heating leads to pronounced changes in temperature and stability in the boundary layer as well as the upper troposphere. This suggests that cloud-radiative heating in the boundary layer and the upper troposphere might affect the cyclone in different ways.

We test this idea by performing additional simulations in which cloud-radiative heating is limited to either the boundary layer (below 2 km) or the free troposphere (above 2 km). The simulations allow us to separate the temperature and stability changes at lower and upper levels (Figures S8, S9 and S10 in Supporting Information S1).

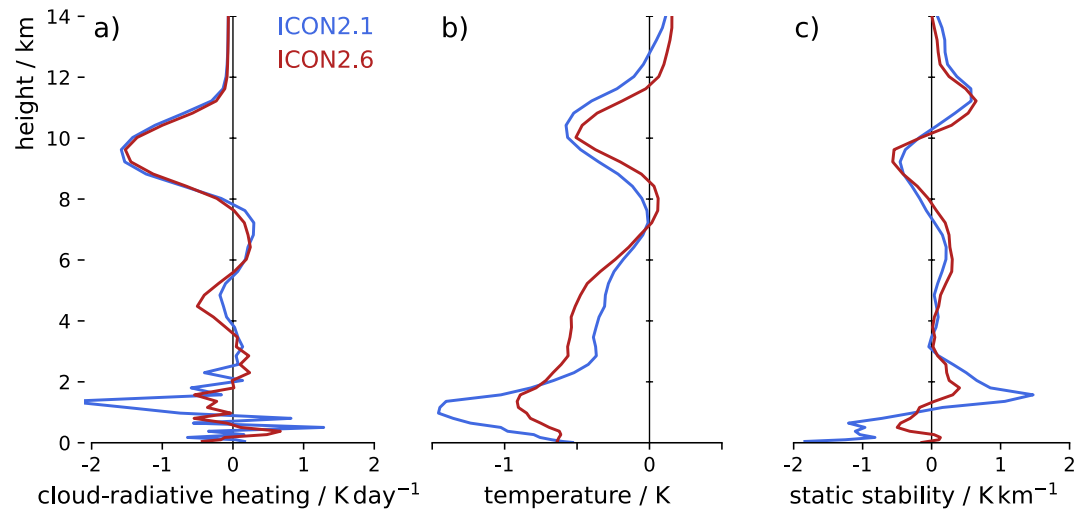


Figure 4. (a) Cloud-radiative heating in the simulations with active cloud-radiative heating. Panels (b) and (c) show the change in temperature and stability in simulations with cloud-radiative heating compared to simulations without radiation. All values are averaged between 40° and 60°N and day 5 and 6.5 over grid boxes with upward motion. The latter are sampled based on the pressure velocity at 5 km height.

The simulations identify a robust tug-of-war between cloud-radiative heating in the free troposphere and the boundary layer (Figure 5). When cloud-radiative heating is limited to the free troposphere, both ICON2.1 and ICON2.6 simulate a stronger cyclone in terms of EKE compared to the no-radiation setup. When only boundary-layer cloud-radiative heating is taken into account, the cyclone weakens in both model versions in terms of EKE as well as cyclone central pressure. Figure 5 further shows that the near-zero cloud-radiative impact on lower-tropospheric EKE and cyclone central pressure in ICON2.6 results from the competing effects of cloud-radiative heating in the free troposphere and the boundary layer.

The tug-of-war also explains why cloud-radiative heating has a different impact on the cyclone in ICON2.1 and ICON2.6. In ICON2.1, the cloud-radiative impact is dominated by the weakening impact of low-level clouds. In contrast, because ICON2.6 simulates fewer low-level clouds, the cloud-radiative impact is dominated by the strengthening impact of high-level clouds.

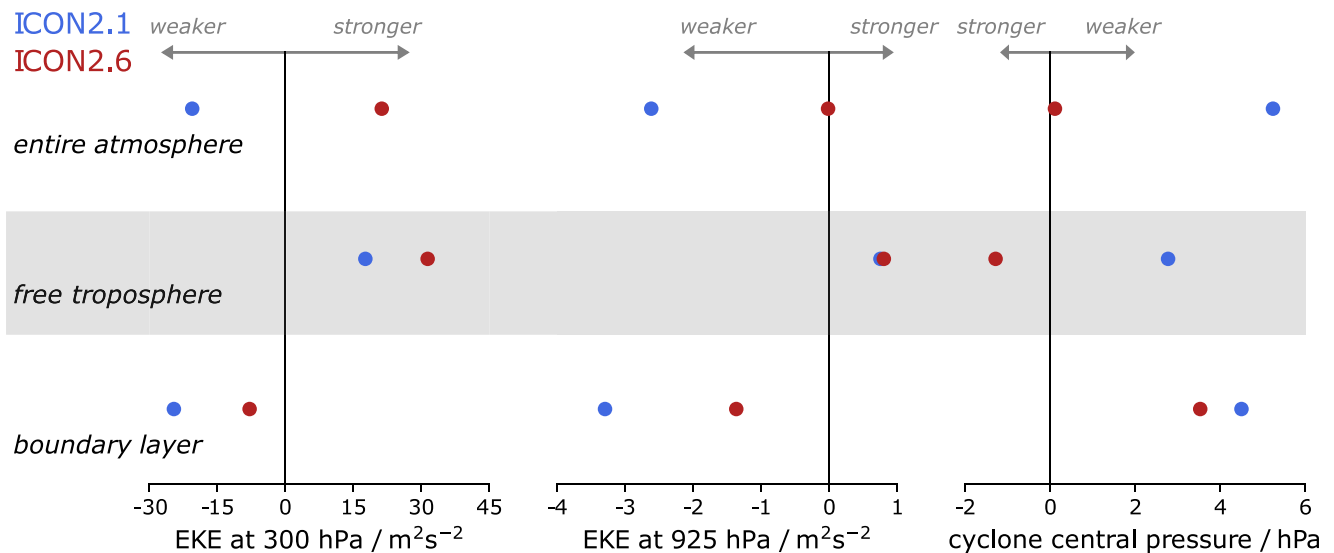


Figure 5. Changes in cyclone intensity due to cloud-radiative heating in the entire atmosphere (top row) and when cloud-radiative heating is limited to the free troposphere (above 2 km; middle row) and the boundary layer (below 2 km; bottom row). The change in cyclone intensity is characterized in terms of the maximum values of eddy kinetic energy (EKE) at 300 and 925 hPa and the minimum value of cyclone central pressure. EKE is averaged between 25° and 75°N. The change in cyclone intensity is calculated as the difference from the simulation without radiation.

3.3. Cloud-Radiative Impact on Static Stability

We now propose that the competing impacts of low-level and high-level cloud-radiative heating can be understood from changes in static stability. We start with the impact of low-level clouds and then discuss the impact of high-level clouds.

The low-level cloud-radiative cooling leads to an increase in static stability around the top of the boundary layer and a decrease below. This low-level dipole in the change of static stability is the expected response to a layer of cooling and leads to a corresponding dipole in PV (Figures S9 and S10, panels c, d, o and p in Supporting Information S1). Based on Boutle et al. (2015), the PV increase near the top of the boundary layer is expected to weaken the coupling between the upper- and lower-levels within the cyclone and thereby reduce the growth rate of the cyclone. An additional and consistent perspective is provided by the Eady model, which predicts that increased static stability results in a weaker cyclone (Eady, 1949; Vallis, 2006).

The high-level cloud-radiative cooling creates a dipole of reduced static stability in the upper-level ridge below the tropopause and enhanced stability above (Figures S9 and S10, panel i in Supporting Information S1). Consistent with the Eady model, the decreased stability enables stronger upward motion in the upper troposphere (not shown) and a stronger cyclone. At the same time, the dipole strengthens the vertical gradient in stability at the tropopause and sharpens the tropopause, which strengthens the upper-level jet (Figures S9 and S10, panels k and l in Supporting Information S1) and works in favor of a stronger cyclone (Boljka & Birner, 2022; Gray et al., 2014).

4. Conclusions

We show that cloud-radiation-interactions affect the dynamics and intensity of an idealized midlatitude cyclone. We perform baroclinic life cycle simulations with two versions of the global atmosphere model ICON that in the past were used by the German Weather Service DWD for operational weather forecasting. Our work continues a line of recent studies that have addressed how cloud-radiative heating of the atmosphere affects the extratropical circulation on synoptic scales. It highlights that cloud-radiation-interactions affect the atmospheric circulation not only on long climatic timescales of years but also on short weather timescales of days to weeks.

We identify a tug-of-war between the radiative heating and cooling of low-level and high-level clouds. In line with Grise et al. (2019), we propose that changes in static stability are key to the cloud-radiative impact and the tug-of-war. Low-level clouds cool the top of the planetary boundary layer by emitting longwave radiation and create a dipole of static stability changes in the lower troposphere. Around the top of the boundary, the static stability increases, which weakens the interaction between the upper-level and lower-level waves and hence weakens the cyclone. High-level clouds also have a cooling effect at their cloud tops by emitting longwave radiation. Yet, the cooling occurs in the upper troposphere and hence decreases tropospheric stability in regions of ascent and sharpens the tropopause. The result is a stronger cyclone. The opposing effects of high-level and low-level clouds reconcile an apparent contradiction between Schäfer and Voigt (2018) and Grise et al. (2019), who concluded that cloud-radiative heating leads to weaker midlatitude cyclones, and Keshtgar et al. (2023), who found that midlatitude cyclones become stronger due to cloud-radiative heating. The contradiction is explained as the result of differences in the simulation of low-level clouds.

Our work shows that the vertical distribution of cloud-radiative heating and cooling can affect idealized midlatitude cyclones. Future work should study how cloud-radiative heating affects “real” cyclones in the midlatitude storm track regions of Earth's atmosphere and how the cloud-radiative impact compares to the impacts of latent heating and cloud microphysics, which are much better understood. We also expect the cloud-radiative impact to differ among cyclones. Finally, future work should address how model biases and shortcomings in the representation of radiative heating from low-level and high-level clouds associated with cyclones (Bodas-Salcedo et al., 2014; Sullivan et al., 2023; Vergara-Temprado et al., 2018) might affect model representations of cyclones and storm tracks.

Data Availability Statement

The simulation output is archived in the Phaidra repository for the permanent secure storage of digital assets at the University of Vienna under <https://doi.org/10.25365/phaidra.407>. The ICON simulation log files and the analysis runscripts are available in the Phaidra repository under <https://doi.org/10.25365/phaidra.408> and via

the GitLab server of the University under <https://gitlab.phaidra.org/climate/voigt-et-al-crh-cyclone-grl2023> (git commit ee9316d7).

The ICON model can be obtained from <https://code.mpimet.mpg.de/projects/iconpublic>. We are grateful to the developers and maintainers of the open source Python packages NumPy (Harris et al., 2020), Xarray (Hoyer & Hamman, 2017) and Matplotlib (Hunter, 2007), which we used for the data analysis.

Acknowledgments

This research was performed within the project B4 of the Transregional Collaborative Research Center SFB/TRR 165 “Waves to Weather” funded by the German Research Foundation (DFG). We thank the German Climate Computing Center (DKRZ, Hamburg) for providing computing and storage resources as part of project bb1135. We are thankful for open access funding provided by the University of Vienna.

References

- Ahmadi-Givi, F. (2002). A review of the role of latent heat release in extratropical cyclones within potential vorticity framework. *Journal of the Earth and Space Physics*, 28(1), 7–20.
- Albern, N., Voigt, A., & Pinto, J. G. (2019). Cloud-radiative impact on the regional responses of the mid-latitude jet streams and storm tracks to global warming. *Journal of Advances in Modeling Earth Systems*, 11(7), 1940–1958. <https://doi.org/10.1029/2018MS001592>
- Albern, N., Voigt, A., & Pinto, J. G. (2021). Tropical cloud-radiative changes contribute to robust climate change-induced jet exit strengthening over Europe during boreal winter. *Environmental Research Letters*, 16(8), 084041. <https://doi.org/10.1088/1748-9326/ac13f0>
- Barker, H. W., Stephens, G. L., Partain, P. T., Bergman, J. W., Bonnel, B., Campana, K., et al. (2003). Assessing 1D atmospheric solar radiative transfer models: Interpretation and handling of unresolved clouds. *Journal of Climate*, 16(16), 2676–2699. [https://doi.org/10.1175/1520-0442\(2003\)016\(2676:ADASRT\)2.0.CO;2](https://doi.org/10.1175/1520-0442(2003)016(2676:ADASRT)2.0.CO;2)
- Bodas-Salcedo, A., Williams, K. D., Ringer, M. A., Beau, I., Cole, J. N. S., Dufresne, J. L., et al. (2014). Origins of the solar radiation biases over the southern ocean in CFMIP2 models. *Journal of Climate*, 27(1), 41–56. <https://doi.org/10.1175/JCLI-D-13-00169.1>
- Boljka, L., & Birner, T. (2022). Potential impact of tropopause sharpness on the structure and strength of the general circulation. *Climate Atmospheric Science*, 5(1), 98. <https://doi.org/10.1038/s41612-022-00319-6>
- Booth, J. F., Wang, S., & Polvani, L. (2013). Midlatitude storms in a moister world: Lessons from idealized baroclinic life cycle experiments. *Climate Dynamics*, 41(3), 787–802. <https://doi.org/10.1007/s00382-012-1472-3>
- Boutle, I. A., Belcher, S. E., & Plant, R. S. (2015). Friction in mid-latitude cyclones: An Ekman-PV mechanism. *Atmospheric Science Letters*, 16(2), 103–109. <https://doi.org/10.1002/asl2.526>
- Box, G. E. P. (1979). Robustness in the strategy of scientific model building. In R. L. Launer & G. N. Wilkinson (Eds.), *Robustness in statistics* (pp. 201–236). Academic Press. <https://doi.org/10.1016/B978-0-12-438150-6.50018-2>
- Ceppi, P., & Hartmann, D. L. (2016). Clouds and the atmospheric circulation response to warming. *Journal of Climate*, 29(2), 783–799. <https://doi.org/10.1175/JCLI-D-15-0394.1>
- Chagnon, J. M., Gray, S. L., & Methven, J. (2013). Diabatic processes modifying potential vorticity in a North Atlantic cyclone. *Quarterly Journal of the Royal Meteorological Society*, 139(674), 1270–1282. <https://doi.org/10.1002/qj.2037>
- Crezee, B., Joos, H., & Wernli, H. (2017). The microphysical building blocks of low-level potential vorticity anomalies in an idealized extratropical cyclone. *Journal of the Atmospheric Sciences*, 74(5), 1403–1416. <https://doi.org/10.1175/JAS-D-16-0260.1>
- Davis, C. A., Stoelinga, M. T., & Kuo, Y.-H. (1993). The integrated effect of condensation in numerical simulations of extratropical cyclogenesis. *Monthly Weather Review*, 121(8), 2309–2330. [https://doi.org/10.1175/1520-0493\(1993\)121<2309:tieoci>2.0.co;2](https://doi.org/10.1175/1520-0493(1993)121<2309:tieoci>2.0.co;2)
- Doms, G., Forstner, J., Heise, E., Herzog, H.-J., Mironov, D., Raschendorfer, M., et al. (2011). *A description of the nonhydrostatic regional COSMO model Part II: Physical parameterization (technical report)*. DWD German Weather Service.
- Eady, E. T. (1949). Long waves and cyclone waves. *Tellus*, 1(3), 33–52. <https://doi.org/10.1111/j.2153-3490.1949.tb01265.x>
- Gray, S. L., Dunning, C. M., Methven, J., Masato, G., & Chagnon, J. M. (2014). Systematic model forecast error in Rossby wave structure. *Geophysical Research Letters*, 41(8), 2979–2987. <https://doi.org/10.1002/2014GL059282>
- Grise, K. M., Medeiros, B., Benedict, J. J., & Olson, J. G. (2019). Investigating the influence of cloud radiative effects on the extratropical storm tracks. *Geophysical Research Letters*, 46(13), 7700–7707. <https://doi.org/10.1029/2019GL083542>
- Grise, K. M., & Polvani, L. M. (2014). Southern Hemisphere cloud-dynamics biases in CMIP5 models and their implications for climate projections. *Journal of Climate*, 27(15), 6074–6092. <https://doi.org/10.1175/JCLI-D-14-00113.1>
- Harris, C. R., Millman, K. J., van der Walt, S. J., Gommers, R., Virtanen, P., Cournapeau, D., et al. (2020). Array programming with NumPy. *Nature*, 585(7825), 357–362. <https://doi.org/10.1038/s41586-020-2649-2>
- Hoyer, S., & Hamman, J. (2017). xarray: N-D labeled arrays and datasets in Python. *Journal of Open Research Software*, 5(1), 10. <https://doi.org/10.5334/jors.148>
- Hunter, J. D. (2007). Matplotlib: A 2D graphics environment. *Computing in Science & Engineering*, 9(3), 90–95. <https://doi.org/10.1109/MCSE.2007.55>
- Kaviani, M., Ahmadi-Givi, F., Mohebalhojeh, A. R., & Yazgi, D. (2022). An assessment of radiative impacts of CO₂ on baroclinic instability using idealized life cycles. *Quarterly Journal of the Royal Meteorological Society*, 148(743), 891–906. <https://doi.org/10.1002/qj.4237>
- Keshtgar, B., Voigt, A., Hoese, C., Riemer, M., & Mayer, B. (2023). Cloud-radiative impact on the dynamics and predictability of an idealized extratropical cyclone. *Weather Climate Dynamics*, 4(1), 115–132. <https://doi.org/10.5194/wcd-4-115-2023>
- Kunkel, D., Hoor, P., Kaluza, T., Ungermann, J., Kluschat, B., Giez, A., et al. (2019). Evidence of small-scale quasi-isentropic mixing in ridges of extratropical baroclinic waves. *Atmospheric Chemistry and Physics*, 19(19), 12607–12630. <https://doi.org/10.5194/acp-19-12607-2019>
- Kunkel, D., Hoor, P., & Wirth, V. (2016). The tropopause inversion layer in baroclinic life cycle experiments: The role of diabatic processes. *Atmospheric Chemistry and Physics*, 16(2), 541–560. <https://doi.org/10.5194/acp-16-541-2016>
- Li, Y., Thompson, D. W. J., & Bony, S. (2015). The influence of atmospheric cloud radiative effects on the large-scale atmospheric circulation. *Journal of Climate*, 28(18), 7263–7278. <https://doi.org/10.1175/JCLI-D-14-00825.1>
- Mlawer, E. J., Taubman, S. J., Brown, P. D., Iacono, M. J., & Clough, S. A. (1997). Radiative transfer for inhomogeneous atmospheres: RRTM, a validated correlated-k model for the longwave. *Journal of Geophysical Research*, 102(D14), 16663–16682. <https://doi.org/10.1029/97jd00237>
- O’Gorman, P. A. (2011). The effective static stability experienced by eddies in a moist atmosphere. *Journal of the Atmospheric Sciences*, 68(1), 75–90. <https://doi.org/10.1175/2010JAS3537.1>
- Pfahl, S., Schwierz, C., Croci-Maspoli, M., Grams, C. M., & Wernli, H. (2015). Importance of latent heat release in ascending air streams for atmospheric blocking. *Nature Geoscience*, 8, 610–614. <https://doi.org/10.1038/ngeo2487>
- Polvani, L. M., & Esler, J. G. (2007). Transport and mixing of chemical air masses in idealized baroclinic life cycles. *Journal of Geophysical Research*, 112(D23), D23102. <https://doi.org/10.1029/2007JD008555>
- Prill, F., Reinert, D., Rieger, D., & Zaengl, G. (2020). *Working with the ICON model (Technical report)*. DWD German Weather Service. <https://doi.org/10.5676/DWDpub/nwv/iconutorial2020>

- Rantanen, M., Räisänen, J., Sinclair, V., & Järvinen, H. (2019). Sensitivity of idealised baroclinic waves to mean atmospheric temperature and meridional temperature gradient changes. *Climate Dynamics*, *52*(5), 2703–2719. <https://doi.org/10.1007/s00382-018-4283-3>
- Rieger, D., Milelli, M., Boucouvala, D., Gofa, F., Iriza-Burca, A., & Khain, P., & the C2I Team. (2021). *Reports on ICON, issue 006: Verification of ICON in limited area mode at COSMO National meteorological services*. (Technical report). Deutscher Wetterdienst. https://doi.org/10.5676/DWD_pub/nwv/icon_006
- Ruppert, J. H., Wing, A. A., Tang, X., & Duran, E. L. (2020). The critical role of cloud–infrared radiation feedback in tropical cyclone development. *Proceedings of the National Academy of Sciences*, *117*(45), 27884–27892. <https://doi.org/10.1073/pnas.2013584117>
- Schäfer, S., & Voigt, A. (2018). Radiation weakens idealized mid-latitude cyclones. *Geophysical Research Letters*, *45*(6), 2833–2841. <https://doi.org/10.1002/2017GL076726>
- Schultz, D. M., Bosart, L. F., Colle, B. A., Davies, H. C., Dearden, C., Keyser, D., et al. (2019). Extratropical cyclones: A century of research on meteorology’s centerpiece. *Meteorological Monographs*, *59*, 16.1–16.56. <https://doi.org/10.1175/AMSMONOGRAPHSD-18-0015.1>
- Shapiro, M. A. & Gronas, S. (Eds.) (1999). *The life cycles of extratropical cyclones*. American Meteorological Society.
- Shaw, T. A., Barnes, E., Baldwin, M., Caballero, R., Garfinkel, C., Hwang, Y.-T., et al. (2016). Storm track processes and the opposing influences of climate change. *Nature Geoscience*, *9*, 656–664. <https://doi.org/10.1038/ngeo2783>
- Sullivan, S., Keshtgar, B., Albern, N., Bala, E., Braun, C., Choudhary, A., et al. (2023). How does cloud-radiative heating over the North Atlantic change with grid spacing, convective parameterization, and microphysics scheme? *Geoscience Model Development*, *16*, 3535–3551. <https://doi.org/10.5194/gmd-16-3535-2023>
- Tierney, G., Posselt, D. J., & Booth, J. F. (2018). An examination of extratropical cyclone response to changes in baroclinicity and temperature in an idealized environment. *Climate Dynamics*, *51*(9–10), 3829–3846. <https://doi.org/10.1007/s00382-018-4115-5>
- Vallis, G. K. (2006). *Atmospheric and oceanic fluid dynamics*. Cambridge University Press.
- Vergara-Temprado, J., Miltenberger, A. K., Furtado, K., Grosvenor, D. P., Shipway, B. J., Hill, A. A., et al. (2018). Strong control of Southern Ocean cloud reflectivity by ice-nucleating particles. *Proceedings of National Academy of Sciences*, *115*(11), 2687–2692. <https://doi.org/10.1073/pnas.1721627115>
- Voigt, A., Albern, N., Ceppi, P., Grise, K., Li, Y., & Medeiros, B. (2021). Clouds, radiation, and atmospheric circulation in the present-day climate and under climate change. *WIREs Climate Change*, *12*(2), e694. <https://doi.org/10.1002/wcc.694>
- Voigt, A., Albern, N., & Papavasileiou, G. (2019). The atmospheric pathway of the cloud-radiative impact on the circulation response to global warming: Important and uncertain. *Journal of Climate*, *32*(10), 3051–3067. <https://doi.org/10.1175/JCLI-D-18-0810.1>
- Voigt, A., & Shaw, T. (2015). Circulation response to warming shaped by radiative changes of clouds and water vapor. *Nature Geoscience*, *8*(2), 102–106. <https://doi.org/10.1038/ngeo2345>
- Volonté, A., Clark, P. A., & Gray, S. L. (2020). Idealised simulations of cyclones with robust symmetrically unstable sting jets. *Weather Climate Dynamics*, *1*(1), 63–91. <https://doi.org/10.5194/wcd-1-63-2020>
- Watt-Meyer, O., & Frierson, D. M. W. (2017). Local and remote impacts of atmospheric cloud radiative effects onto the eddy-driven jet. *Geophysical Research Letters*, *44*(19), 10036–10044. <https://doi.org/10.1002/2017GL074901>
- Zängl, G. (2021). Operationelles NWV-system: ICON: Model configuration upgrade of ICON (Gültigkeit ab 14.04.2021) (Technical report). DWD. Retrieved from https://www.dwd.de/DE/fachnutzer/forschung_lehre/numerische_wettervorhersage/nwv_aenderungen/_functions/DownloadBox_modellaenderungen/icon/pdf_2021/pdf_icon_14_04_2021.pdf
- Zängl, G., & Paul, G. (2016). ICON: ICON-modellsystem mit der Einführung der Modellversion 2.0.15 (Gültigkeit ab 28.09.2016) (Technical report). DWD. Retrieved from https://www.dwd.de/DE/fachnutzer/forschung_lehre/numerische_wettervorhersage/nwv_aenderungen/_functions/DownloadBox_modellaenderungen/icon/pdf_2016/pdf_icon_28_09_2016.pdf
- Zängl, G., Reinert, D., Ripodas, P., & Baldauf, M. (2015). The ICON (ICOsahedral Non-hydrostatic) modelling framework of DWD and MPI-M: Description of the non-hydrostatic dynamical core. *Quarterly Journal of the Royal Meteorological Society*, *141*(687), 563–579. <https://doi.org/10.1002/qj.2378>
- Zängl, G., & Schäfer, S. (2021). Operational NWP system: Model configuration upgrade of ICON (Technical report). Retrieved from https://www.dwd.de/DE/fachnutzer/forschung_lehre/numerische_wettervorhersage/nwv_aenderungen/_functions/DownloadBox_modellaenderungen/icon/pdf_2021/pdf_icon_14_04_2021.pdf